High Power Laser Science and Engineering, (2020), Vol. 8, e21, 8 pages.
doi:10.1017/hpl.2020.22

HIGH POWER LASER SCIENCE AND ENGINEERING

RESEARCH ARTICLE

Stimulated Raman scattering in a non-eigenmode regime

Yao Zhao[1], Suming Weng[2,3], Zhengming Sheng[2,3,4], and Jianqiang Zhu[1,3]

[1]*Key Laboratory of High Power Laser and Physics, Shanghai Institute of Optics and Fine Mechanics, Chinese Academy of Sciences, Shanghai 201800, China*

[2]*Key Laboratory for Laser Plasmas (MoE), School of Physics and Astronomy, Shanghai Jiao Tong University, Shanghai 200240, China*

[3]*Collaborative Innovation Center of IFSA (CICIFSA), Shanghai Jiao Tong University, Shanghai 200240, China*

[4]*SUPA, Department of Physics, University of Strathclyde, Glasgow G4 0NG, UK*

(Received 6 April 2020; revised 21 April 2020; accepted 24 April 2020)

Abstract

Stimulated Raman scattering (SRS) in plasma in a non-eigenmode regime is studied theoretically and numerically. Different from normal SRS with the eigen electrostatic mode excited, the non-eigenmode SRS is developed at plasma density $n_e > 0.25n_c$ when the laser amplitude is larger than a certain threshold. To satisfy the phase-matching conditions of frequency and wavenumber, the excited electrostatic mode has a constant frequency around half of the incident light frequency $\omega_0/2$, which is no longer the eigenmode of electron plasma wave ω_{pe}. Both the scattered light and the electrostatic wave are trapped in plasma with their group velocities being zero. Super-hot electrons are produced by the non-eigen electrostatic wave. Our theoretical model is validated by particle-in-cell simulations. The SRS driven in this non-eigenmode regime is an important laser energy loss mechanism in the laser plasma interactions as long as the laser intensity is higher than 10^{15} W/cm^2.

Keywords: hot electrons; laser plasma interactions; stimulated Raman scattering

1. Introduction

Laser plasma interactions (LPIs) are widely associated with many applications such as inertial confinement fusion (ICF)[1–3], radiation sources[4], plasma optics[5, 6] and laboratory astrophysics[7, 8]. The concomitant parametric instabilities found in LPI are nonlinear processes, which can greatly affect the outcome[9]. Generally, laser plasma instabilities[10, 11], especially stimulated Raman scattering (SRS), stimulated Brillouin scattering (SBS) and two-plasmon decay (TPD) instability, have been mainly considered in ICF with the incident laser intensity less than 10^{15} W/cm^2[12–14]. However, the laser intensity may be of the order of 10^{16} or even 10^{17} W/cm^2 in shock ignition[15–19], Brillouin amplification[20, 21] and the interactions of high-power laser with matter[22–24]. Therefore, the parametric instabilities close to the regime of subrelativistic intensity need to be explored in depth.

As well known, SRS usually develops in plasma density not larger than the quarter critical density $n_e \leqslant 0.25n_c$ due to the decay of the scattering light in its propagation in the overdense density plasma[4, 10]. In the density region $n_e \leqslant 0.25n_c$, the electrostatic wave is the eigenmode of the electron plasma wave. Relativistic intensity lasers can reduce the effective electron plasma frequency, and therefore eigenmode SRS may develop at $n_e > 0.25n_c$[25]. In this work, we show the presence of non-eigenmode SRS, which is found at plasma density $n_e > 0.25n_c$ even without considering the relativistic effect. The development of a non-eigen electrostatic mode is described by the linear perturbations of fluid equations, which may lead to a few subsequent nonlinear phenomena[20, 26–28]. This mode develops only when the laser intensity exceeds a certain threshold. The theoretical model is supported by particle-in-cell (PIC) simulations.

2. Theoretical analysis of SRS in the non-eigenmode regime

Generally, SRS is a three-wave instability where a laser decays into an electrostatic wave, with frequency equal to the eigen electron plasma wave, and a light wave. However, the

Correspondence to: Y. Zhao, No. 390 Qinghe Road, Jiading District, Shanghai 201800, China. Email: yaozhao@siom.ac.cn

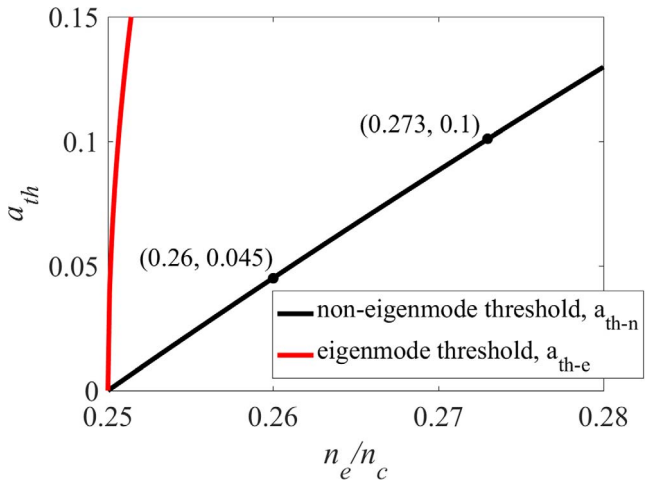

Figure 1. Amplitude thresholds for the development of eigenmode and non-eigenmode SRS in plasma above the quarter critical density. The threshold for the case of eigenmode SRS a_{th-e} is due to the relativistic effect.

stimulated electrostatic wave is no longer the eigenmode of the electron plasma wave in the SRS non-eigenmode regime, where both the frequencies of scattered light and electrostatic field are nearly half of the incident laser frequency. The mechanism of this instability can be described by the SRS dispersion relation at plasma density $n_e > 0.25n_c$.

To investigate the non-eigenmode SRS mechanism in LPI, we first introduce the non-relativistic dispersion relation of SRS in cold plasma[10]

$$\omega_e^2 - \omega_{pe}^2 = \frac{\omega_{pe}^2 k_e^2 c^2 a_0^2}{4}\left(\frac{1}{D_{e+}} + \frac{1}{D_{e-}}\right), \tag{1}$$

where $D_{e\pm} = \omega_e^2 - k_e^2c^2 \mp 2(k_0k_ec^2 - \omega_0\omega_e)$ and a_0 is the laser normalized amplitude. The relation between laser intensity I and a_0 is given by $I\,(\mathrm{W/cm^2}) = 1.37 \times 10^{18} a_0^2/[\lambda(\mu\mathrm{m})]^2$. Furthermore, in Equation (1), ω_0 and ω_e are the frequencies of the incident laser and the electrostatic wave, respectively. k_0 and k_e are the wavenumbers of the pump laser and the electrostatic wave, respectively. Generally, we have $\mathrm{Re}(\omega_e) = \omega_{pe}$ in the SRS eigenmode regime $n_e \leqslant 0.25n_c$. However, when the amplitude of the incident laser a_0 is larger than a threshold, a stimulated non-eigen electrostatic mode $\mathrm{Re}(\omega_e) \neq \omega_{pe}$ will be developed at $n_e > 0.25n_c$.

Now we analytically solve Equation (1) under $n_e > 0.25n_c$. Let $\omega_e = \omega_{er} + i\omega_{ei}$, where ω_{er} and ω_{ei} are the real and imaginary parts of ω_e, respectively. The wavenumber of scattering light is a real $k_sc = 0$ in the non-eigenmode regime, i.e., the scattered light is trapped in the plasma. And to keep the phase-matching conditions, we set the electrostatic wavenumber $k_ec = k_0c$. In this case, the imaginary part of Equation (1) can be simplified to

$$\begin{aligned}(\omega_0\omega_{ei} - 2\omega_{ei}\omega_{er})\,(\omega_{ei}^2 - \omega_{er}^2 - 2\omega_0\omega_{er} + 3\omega_0^2 \\ - 3\omega_{pe}^2)(\omega_{er}^2 + \omega_{ei}^2 - \omega_{er}\omega_0 - \omega_{pe}^2) = 0.\end{aligned} \tag{2}$$

Equation (2) is satisfied for any ω_{pe} when $\omega_{er} = \omega_0/2$. Therefore, the frequency of the electrostatic wave is a constant, and it is independent of the plasma density. The phase velocity of the electrostatic wave is around $v_{ph} = \omega_{er}/k_e \gtrsim c/\sqrt{3} \sim 0.58c$.

Substituting $\omega_{er} = \omega_0/2$ into the real part of Equation (1), one obtains the growth rate of the SRS non-eigenmode:

$$\omega_{ei} = \frac{1}{2}\sqrt{4\omega_{pe}(\omega_0 - \omega_{pe}) + \omega_{pe}^2 a_0^2 k_0^2 c^2/\omega_0^2 - \omega_0^2}. \tag{3}$$

The above equation indicates that the growth rate ω_{ei} is reduced by the increase in plasma density. The threshold a_{th-n} for SRS developing in the non-eigenmode regime can be obtained from $4\omega_{pe}(\omega_0 - \omega_{pe}) + \omega_{pe}^2 a_{th-n}^2 k_0^2 c^2/\omega_0^2 - \omega_0^2 \gtrsim 0$, i.e.,

$$a_{th-n} \gtrsim \frac{\omega_0\sqrt{\omega_0^2 + 4(\omega_{pe}^2 - \omega_{pe}\omega_0)}}{\omega_{pe}k_0c}. \tag{4}$$

Equation (4) indicates that $0.25n_c$ is the turning point between eigenmode SRS and non-eigenmode SRS, where the threshold $a_{th-n} = 0$.

For the density region just near the quarter critical density $n_e \gtrsim 0.25n_c$, Equation (4) can be simplified to $a_{th-n} \gtrsim (8/\sqrt{3})(n_e/n_c - 0.25)$. Therefore, the condition for the excitation of non-eigenmode SRS in a plasma with density $n_e \gtrsim 0.25n_c$ is that the amplitude of pump laser satisfies the above condition, which is almost linearly proportional to the plasma density.

In the following, we consider the relativistic modification of the SRS non-eigenmode in hot plasma. The dispersion of SRS under the relativistic intensity laser is[9, 25]

$$\omega_e^2 - \omega_L^2 = \frac{\omega_{pe}'^2 k_e^2 c^2 a_0^2}{4\gamma^2}\left(\frac{1}{D_{e+}} + \frac{1}{D_{e-}}\right), \tag{5}$$

where $\omega_L^2 = \omega_{pe}'^2 + 3k_e^2v_{th}^2$ with $\omega_{pe}' = \omega_{pe}/\sqrt{\gamma}$, and $\gamma = (1 + a_0^2/2)^{1/2}$ and v_{th} are the relativistic factor and electron thermal velocity, respectively. Different from non-eigenmode SRS, the threshold for eigenmode SRS developing in cold plasma with $n_e > 0.25n_c$ is $\omega_{pe}' \leqslant 0.5\omega_0$, i.e., $a_{th-e} \geqslant \sqrt{2(16n_e^2/n_c^2 - 1)}$. As a comparison, the driven amplitudes for non-eigenmode SRS a_{th-n} and eigenmode SRS a_{th-e} at different plasma densities are shown in Figure 1. One finds that the amplitude threshold for eigenmode SRS is much larger than for non-eigenmode SRS, i.e., $a_{th-e} \gg a_{th-n}$. Therefore, the intensity of SRS in $n_e > 0.25n_c$ is underestimated according to the previous eigenmode model. As an example, the threshold for laser driving non-eigenmode SRS at plasma density $n_e = 0.26n_c$ is around $a_{th-n} = 0.045$. A laser with amplitude $a_0 = 0.1$ can develop non-eigenmode SRS in the plasma region with density $0.25n_c < n_e \lesssim 0.273n_c$.

https://doi.org/10.1017/hpl.2020.22 Published online by Cambridge University Press

Following the similar steps of the non-relativistic case, the imaginary part of Equation (5) is simplified to

$$(\omega_0\omega_{ei} - 2\omega_{ei}\omega_{er})\,(\omega_{ei}^2 - \omega_{er}^2 - 2\omega_0\omega_{er} + 3\omega_0^2 - 3\omega_{pe}'^2)(\omega_{er}^2 + \omega_{ei}^2 - \omega_{er}\omega_0 - \omega_L^2) = 0. \quad (6)$$

We obtain the same identical relation for the real part $\omega_{er} = \omega_0/2$ from Equation (6). Note that the relativistic factor and electron temperature have no effect on ω_{er} which is no longer the eigen frequency ω_L. The dispersion relation of the non-eigen electrostatic mode satisfies

$$\omega_{er} = \frac{\omega_0}{2} = \frac{1}{2}\sqrt{k_e^2c^2 + \omega_{pe}^2}. \quad (7)$$

From Equation (7), we know that the group velocity of non-eigen electrostatic wave is $v_g = \delta\omega_{er}/\delta k_e \approx 0$. Therefore, electrostatic wave will be trapped in the plasma.

The comparisons between the numerical solutions of Equations (1) and (5) are exhibited in Figure 2. One finds that $\mathrm{Re}(\omega_e) = \omega_0/2$ is a constant even including relativistic and temperature effects. The frequency of electron plasma wave is reduced by the relativistic factor $\omega_{pe}' = \omega_{pe}/\sqrt{\gamma}$. Therefore, the growth rate ω_{ei} is increased by the relativistic modification as shown in Figure 2(a). On the contrary, the frequency of electron plasma wave is enhanced by the electron temperature $\omega_L = \sqrt{\omega_{pe}'^2 + 3k_e^2v_{th}^2}$, and therefore we find a decrease of the growth rate at higher temperature $T_e = 1$ keV in Figure 2(b). Note that the above studies are discussed in the weak relativistic regime, where the plasma density modulation induced by the laser ponderomotive force is weak.

Phase-matching conditions are satisfied in the SRS non-eigenmode regime, and therefore the frequency of concomitant light is also $\mathrm{Re}(\omega_s) \approx 0.5\omega_0$, which can be obtained from the dispersion relation of scattered light

$$\omega_s^2 - k_s^2c^2 - \omega_{pe}^2 = D_{s+} + D_{s-}, \quad (8)$$

where $D_{s\pm} = \omega_{pe}^2(k_s \pm k_0)^2c^2a_0^2/4[(\omega_s \pm \omega_0)^2 - \omega_{pe}^2]$.

According to the linear parametric model of inhomogeneous plasma, the Rosenbluth gain saturation coefficient for convective instability is $G = 2\pi\Gamma^2/v_sv_pK'$[29], where Γ, v_s and v_p are the instability growth rate, the group velocity of scattering light and the plasma wave, respectively. K is the wavenumber mismatch for incident light, scattering light and plasma wave. As it is known, convective instability transits to absolute instability when $K = 0$[30]. Based on the above discussions, the mismatching term of non-eigenmode SRS is $K_{ne} = k_0 - k_e - k_s = 0$ due to $k_e = k_0$ and $k_s = 0$ all the time. Therefore, non-eigenmode SRS is an absolute instability in inhomogeneous plasma.

In conclusion, different from normal SRS, a new type of non-eigenmode SRS can develop in plasma with density $n_e > 0.25n_c$. The stimulated electrostatic mode has an almost constant frequency around half of the incident light frequency $\omega_0/2$, which is no longer the eigenmode of the electron plasma wave ω_{pe}. The group velocities of concomitant light and electrostatic wave are zero in the non-eigenmode regime. The non-eigenmode SRS develops only when the laser intensity is higher than a certain threshold, which is related to the plasma density.

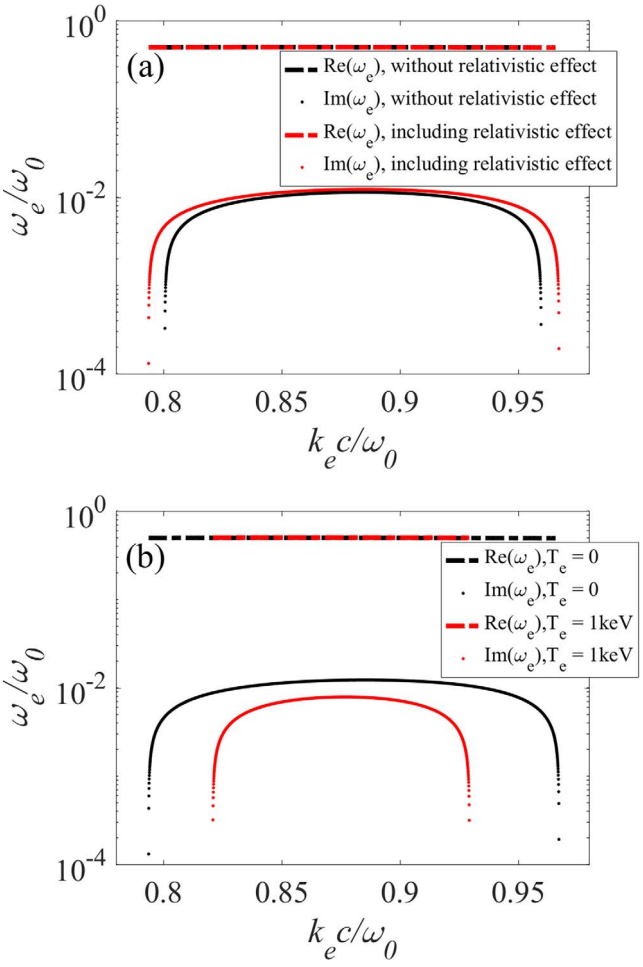

Figure 2. Numerical solutions of SRS dispersion equation at plasma density $n_e = 0.27n_c$ with laser amplitude $a_0 = 0.1$. (a) The relativistic modification on the non-eigenmode SRS at $T_e = 0$. (b) The effect of electron temperature on non-eigenmode SRS. The dotted line and dashed line are the imaginary part and the real part of the solutions, respectively.

3. Simulations for non-eigenmode SRS excitation

3.1. One-dimensional simulations for non-eigenmode SRS in homogeneous plasma

To validate the analytical predictions for non-eigenmode SRS, we have performed several one-dimensional simulations by using the OSIRIS code[31, 32]. The space and time given in the following are normalized by the laser wavelength in vacuum λ and the laser period τ. A linearly

https://doi.org/10.1017/hpl.2020.22 Published online by Cambridge University Press

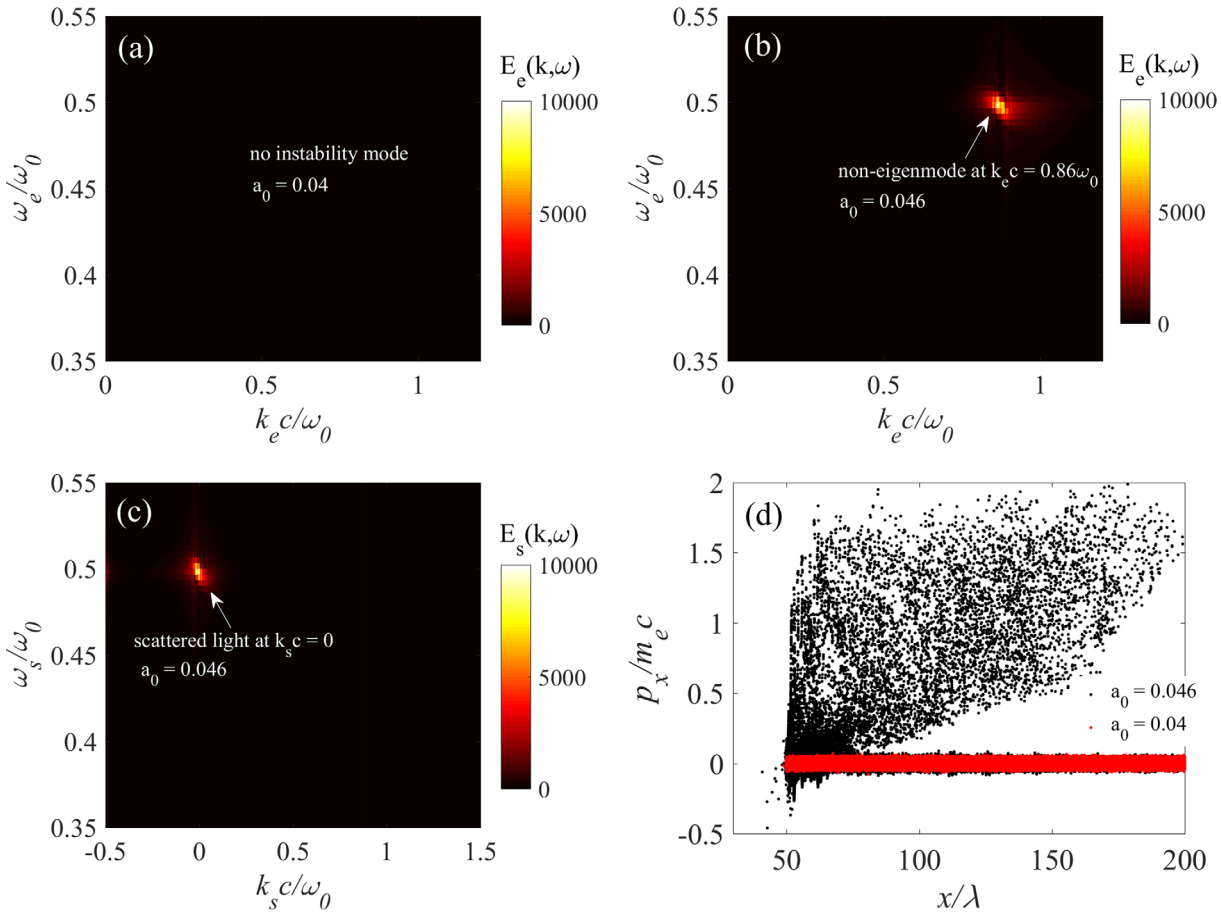

Figure 3. Distributions of the electrostatic wave in (k_e, ω_e) space obtained for the time window $[100\tau, 400\tau]$ at plasma density $n_e = 0.26n_c$ under (a) pump laser amplitude $a_0 = 0.04$ and (b) pump laser amplitude $a_0 = 0.046$. (c) Distribution of the electromagnetic wave in (k_s, ω_s) space obtained under the same conditions as in (b). (d) Longitudinal phase space distribution of electrons under different laser amplitudes at $t = 600\tau$.

polarized semi-infinite pump laser with a uniform amplitude is incident from the left boundary of the simulation box. In this subsection, only the fluid property of the instability is considered, and therefore we set electron temperature $T_e = 100$ eV with immobile ions. The plasma density is $n_e = 0.26n_c$.

Based on Equation (4) and Figure 1, we know that the triggering threshold for non-eigenmode SRS is $a_{th-n} = 0.045$ at density $n_e = 0.26n_c$. To validate the theoretical threshold, two simulation examples under different laser intensities are displayed here. Figure 3(a) shows the case when the laser amplitude is less than the threshold ($a_0 = 0.04 < 0.045$), and no instability mode can be found. When the laser amplitude is increased to $a_0 = 0.046 > 0.045$, the non-eigen electrostatic mode can be found at $k_e c \approx 0.86\omega_0$ and $\omega_e \approx 0.499\omega_0$ in Figure 3(b). The corresponding electromagnetic mode with $k_s c \approx 0$ and $\omega_s \approx 0.5\omega_0$ is shown in Figure 3(c). These simulation results agree well with the analytical prediction. As discussed above, the phase velocity of the non-eigen electrostatic wave is around $v_{ph} \sim 0.58c$ at $n_e = 0.26n_c$. Therefore, numbers of electrons are heated enormously at the nonlinear stage $t \gtrsim 600\tau$ in the SRS non-eigenmode regime as compared to the case below the threshold as shown in Figure 3(d).

3.2. Two-dimensional simulations for non-eigenmode SRS in homogeneous plasma

To further validate the linear development and nonlinear evolution of non-eigenmode SRS in high-dimensionality with mobile ions, we have performed several two-dimensional simulations. The plasma occupies a longitudinal region from 25λ to 125λ and a transverse region from 5λ to 25λ with homogeneous density $n_e = 0.26n_c$. The initial electron temperature is $T_e = 100$ eV. Ions are movable with mass $m_i = 3672m_e$ and an effective charge $Z = 1$. An s-polarized (electric field of light is perpendicular to the simulation plane) semi-infinite pump laser with a peak amplitude $a_0 = 0.05$ at focal plane $x = 75\lambda$ is incident from the left boundary of the simulation box.

According to Equation (4), we know that the incident laser with peak amplitude $a_0 = 0.05$ is sufficient to develop non-eigenmode SRS at plasma density $n_e = 0.26n_c$.

https://doi.org/10.1017/hpl.2020.22 Published online by Cambridge University Press

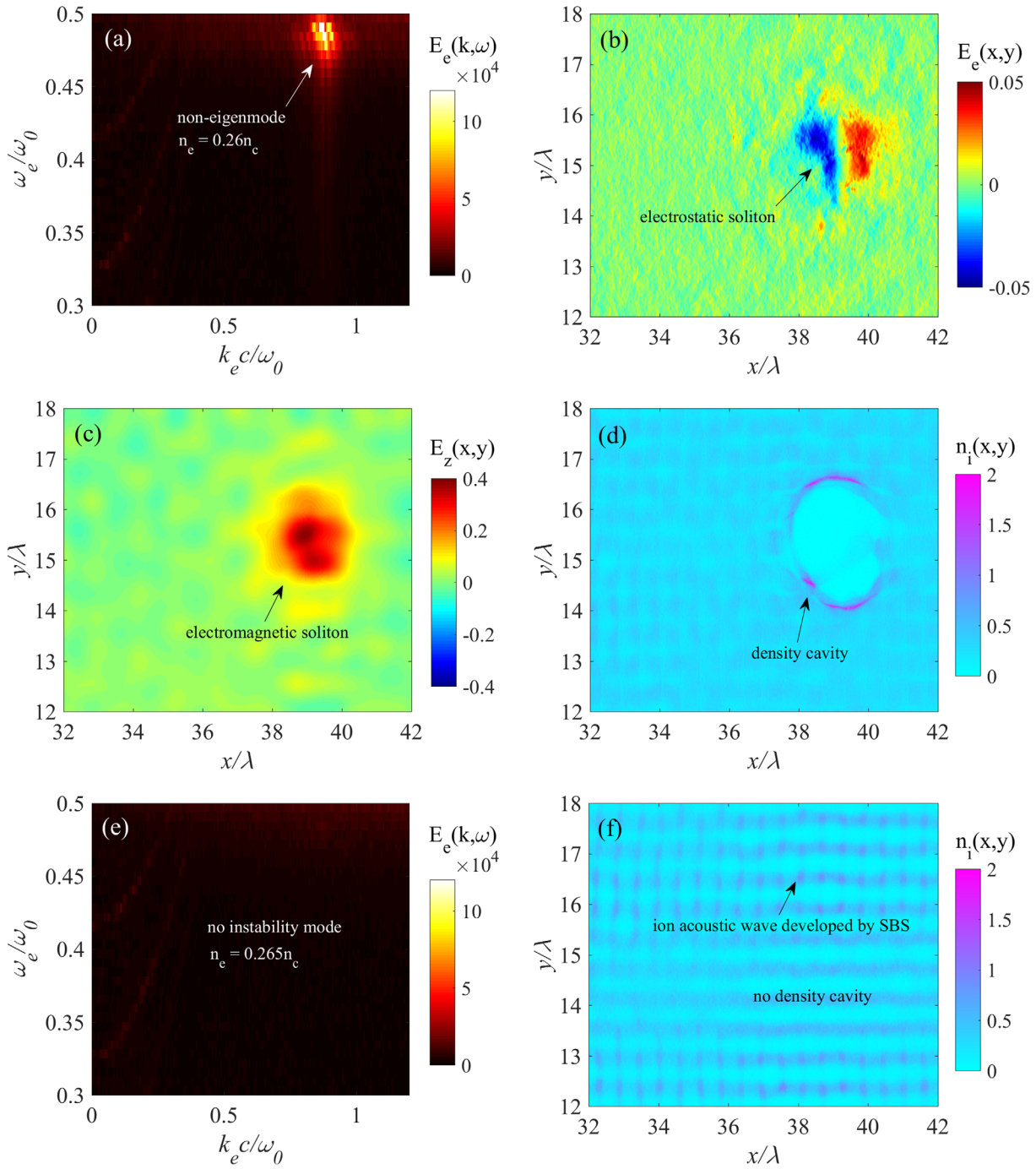

Figure 4. The plasma density is $n_e = 0.26n_c$ for (a)–(d). (a) Distribution of the electrostatic wave in (k_e, ω_e) space obtained for the time window $[320\tau, 480\tau]$ and transverse region $[14.4\lambda, 15.6\lambda]$. (b) Spatial distribution of electrostatic wave at $t = 1850\tau$. (c) Spatial distribution of electromagnetic wave at $t = 1850\tau$. (d) Spatial distribution of ion density at $t = 1950\tau$. The plasma density is $n_e = 0.265n_c$ for (e) and (f). (e) Distribution of the electrostatic wave in (k_e, ω_e) space obtained for the time window $[320\tau, 480\tau]$ and transverse region $[14.4\lambda, 15.6\lambda]$. (f) Spatial distribution of the ion density at $t = 1950\tau$. E_e and E_z are normalized by $m_e\omega_0 c/e$, where m_e and e respectively are the electron mass and electron charge. n_i is normalized by n_c.

The simulation results for plasma density $n_e = 0.26n_c$ are displayed in Figures 4(a)–4(d). Fourier transform of the electrostatic wave is taken for the time window $[320\tau, 480\tau]$. We summate the Fourier spectrum along the transverse direction between $y = 14.4\lambda$ and $y = 15.6\lambda$, and show the distribution in Figure 4(a). One can find a non-eigen electrostatic mode around $k_e c = 0.86\omega_0$ and $\omega_e = 0.492\omega_0$. Note that the growth rate of SBS is about half of the non-eigenmode SRS; therefore, SBS has little effect on the development of non-eigenmode SRS. As discussed in Section 2, the group velocities of the electrostatic wave and electromagnetic wave associated with the non-eigenmode

https://doi.org/10.1017/hpl.2020.22 Published online by Cambridge University Press

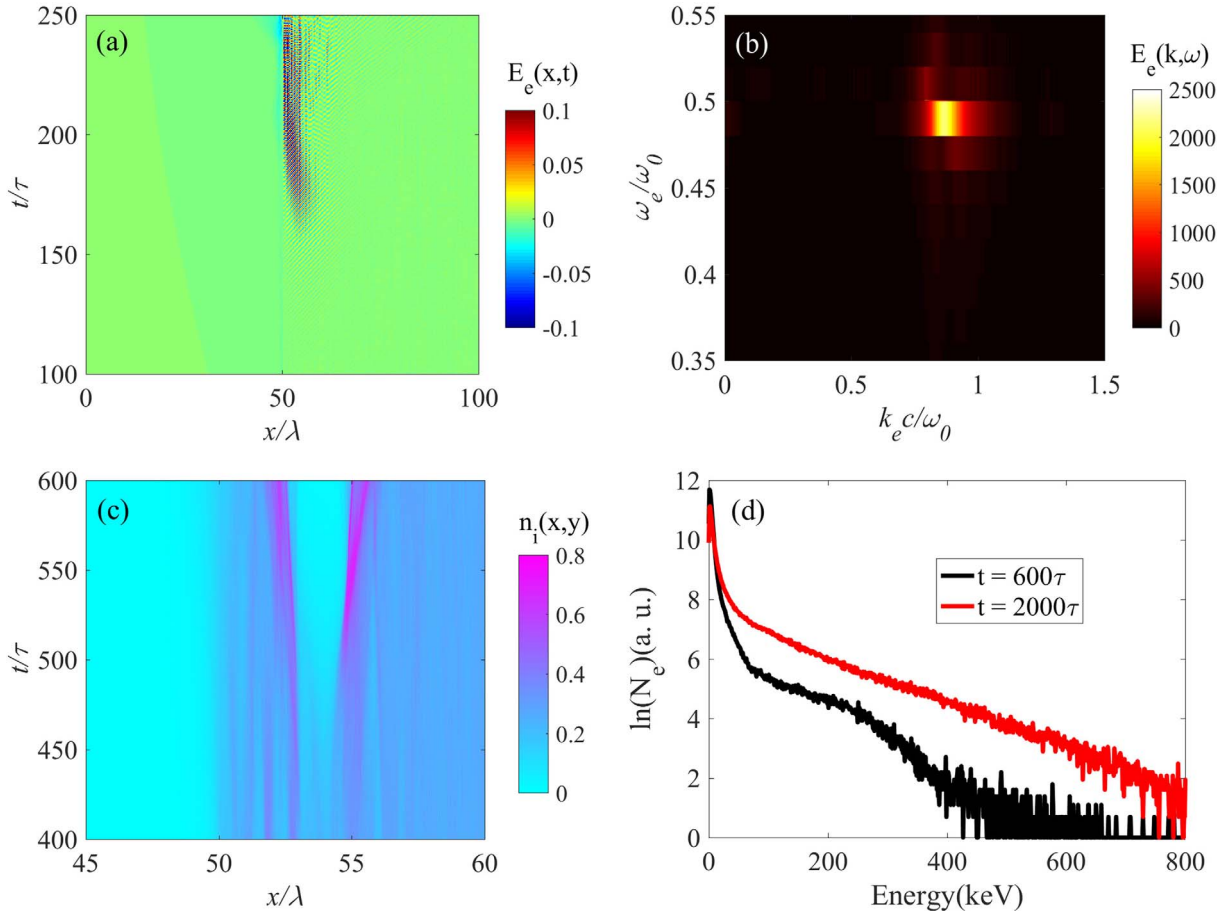

Figure 5. (a) The spatial–temporal distributions of electrostatic wave. (b) Distributions of the electrostatic wave in (k_e, ω_e) space obtained for the time window $[150\tau, 200\tau]$. (c) The spatial–temporal distributions of ion density. (d) Energy distributions of electrons at different times. E_e and n_i respectively are normalized by $m_e\omega_0 c/e$ and n_c.

SRS are zero. As a result, they will be trapped in the plasma. This is confirmed in our numerical simulation as shown in Figures 4(b) and 4(c) that the electrostatic wave and the concomitant electromagnetic wave form localized structures. The trapped light and electrostatic wave may cause the laser energy deficit in ICF related experiments[33]. The trapped waves expel the ions to form density cavity at later time $t = 1950\tau$ as seen from Figure 4(d). These plasma cavities subsequently affect the evolution of the non-eigenmode SRS and SBS[20, 27, 28]. Note that this density cavity is formed due to the non-eigenmode SRS, which is different from the solitons generated by relativistic intensity lasers[34–38].

The laser with peak amplitude $a_0 = 0.05 < a_{th-n} = 0.067$ is insufficient to develop non-eigenmode SRS at $n_e = 0.265n_c$. The simulation results under plasma density $n_e = 0.265n_c$ are displayed in Figures 4(e) and 4(f). The comparison between Figures 4(a) and 4(e) indicates that the pump laser with peak amplitude $a_0 = 0.05$ fails to drive non-eigenmode SRS at $n_e = 0.265n_c$ when the amplitude threshold is not reached. Only the ion acoustic wave developed by SBS with wavenumber $k_i c = 2k_0 c = 1.72\omega_0$ can be found in Figure 4(f). And no density cavities have been formed under the conditions. These results further indicate that non-eigenmode SRS is a seed for the subsequent nonlinear physical phenomena.

3.3. One-dimensional simulations for non-eigenmode SRS in inhomogeneous plasma

To study the non-eigenmode SRS in hot inhomogeneous plasma, we have performed a simulation for the inhomogeneous plasma $n_e = 0.26\exp[(x - 50)/1000]n_c$ with density range $[0.26n_c, 0.287n_c]$. The plasma locates in $x = [50\lambda, 150\lambda]$, and two 50λ vacuums are left on either side of the plasma. The initial electron temperature is $T_e = 2$ keV. Ions are movable with mass $m_i = 3672m_e$. The ion charge and temperature respectively are $Z = 1$ and $T_i = 1$ keV. The driving laser is a linearly polarized semi-infinite pump laser with a uniform amplitude $a_0 = 0.07$.

The spatial–temporal evolution of the electrostatic wave is exhibited in Figure 5(a). We find that a strong electrostatic wave has been developed at the front of plasma $x \lesssim 60\lambda$

https://doi.org/10.1017/hpl.2020.22 Published online by Cambridge University Press

at $t = 180\tau$. The electrostatic wave envelop is found to be stationary due to its group velocity $v_g = 0$. Note that the spatial gradient has little effect on the development of non-eigenmode SRS, in that the phase matching of the three waves is always satisfied in inhomogeneous plasma. Therefore, non-eigenmode SRS is an absolute instability. Figure 5(b) shows the distribution of electrostatic wave in (k_e, ω_e) space, where one can find a spectrum around $\omega_e = 0.499\omega_0$. This result further validates that the frequency of non-eigen electrostatic wave is independent of plasma density and electron temperature. The electrostatic and electromagnetic waves trapped in plasma will expel ions. From Figure 5(c), we know that the ion density cavity is gradually formed from $t = 400\tau$ at the front of plasma. Large numbers of hot electrons are produced by the non-eigen electrostatic field as shown in Figure 5(d). As discussed above, the phase velocity of the non-eigen electrostatic field is around $0.58c$. The temperature of the electron hot tail at $t = 2000\tau$ is around 141 keV. The transmission rate of the pump laser through plasma is about 19.46% at $t = 2000\tau$, which indicates that non-eigenmode SRS is an important pump energy loss mechanism in the LPI as long as the laser intensity is higher than 10^{15} W/cm^2.

4. Summary

In summary, we have shown theoretically and numerically that the non-eigenmode SRS develops at plasma density $n_e > 0.25n_c$ when the laser amplitude is larger than a certain threshold. The electrostatic wave produced by the non-eigenmode SRS has a constant frequency $\omega_0/2$, which is no longer the eigen electron plasma wave ω_{pe}. The phase velocity of the non-eigen electrostatic wave is about $0.58c$, which corresponds to an electron energy of 175 keV. Therefore, super-hot electrons can be produced via the development of the non-eigenmode SRS. The trapped electromagnetic wave and electrostatic wave associated with this instability can drive density cavities in plasma. Our theoretical model is validated by PIC simulations. The non-eigenmode SRS is an important pump energy loss mechanism in the LPI as long as the laser intensity is higher than 10^{15} W/cm^2.

Acknowledgements

This work was supported by the Natural Science Foundation of Shanghai (No. 19YF1453200), the Strategic Priority Research Program of Chinese Academy of Sciences (Nos. XDA25050800 and XDA25050100), the National Natural Science Foundation of China (Nos. 11775144 and 1172109), and the National Science and Technology Innovation Foundation of the Chinese Academy of Sciences (No. CXJJ-20S015). The authors would like to acknowledge the OSIRIS Consortium, consisting of UCLA and IST (Lisbon, Portugal), for providing access to the OSIRIS 4.0 framework.

References

1. E. M. Campbell, V. N. Goncharov, T. C. Sangster, S. P. Regan, P. B. Radha, R. Betti, J. F. Myatt, D. H. Froula, M. J. Rosenberg, and I. V. Igumenshchev, Matter Radiat. Extrem. **2**, 37 (2017).
2. D. Froula, L. Divol, R. London, R. Berger, T. Döppner, N. Meezan, J. Ralph, J. Ross, L. Suter, and S. Glenzer, Phys. Plasmas **17**, 056302 (2010).
3. J. F. Myatt, J. Zhang, R. W. Short, A. V. Maximov, W. Seka, D. H. Froula, D. H. Edgell, D. T. Michel, I. V. Igumenshchev, D. E. Hinkel, P. Michel, and J. D. Moody, Phys. Plasmas **21**, 055501 (2014).
4. C. S. Liu, V. K. Tripathi, and B. Eliasson, *High-power Laser-plasma Interaction* (Cambridge University Press, 2019).
5. L. Lancia, A. Giribono, L. Vassura, M. Chiaramello, C. Riconda, S. Weber, A. Castan, A. Chatelain, A. Frank, and T. Gangolf, Phys. Rev. Lett. **116**, 075001 (2016).
6. G. Lehmann and K. H. Spatschek, Phys. Plasmas **20**, 073112 (2013).
7. R. P. Drake, *High-energy-density Physics: Fundamentals, Inertial Fusion, and Experimental Astrophysics* (Springer Science and Business Media, 2006).
8. K. Falk, High Power Laser Sci. Eng. **6**, e59 (2018).
9. P. Gibbon, *Short Pulse Laser Interactions with Matter* (World Scientific Publishing Company, 2004).
10. W. L. Kruer, *The Physics of Laser Plasma Interactions* (Addison-Wesley, 1988).
11. D. S. Montgomery, Phys. Plasmas **23**, 055601 (2016).
12. R. S. Craxton, K. S. Anderson, T. R. Boehly, V. N. Goncharov, D. R. Harding, J. P. Knauer, R. L. McCrory, P. W. McKenty, D. D. Meyerhofer, J. F. Myatt, A. J. Schmitt, J. D. Sethian, R. W. Short, S. Skupsky, W. Theobald, W. L. Kruer, K. Tanaka, R. Betti, T. J. B. Collins, J. A. Delettrez, S. X. Hu, J. A. Marozas, A. V. Maximov, D. T. Michel, P. B. Radha, S. P. Regan, T. C. Sangster, W. Seka, A. A. Solodov, J. M. Soures, C. Stoeckl, and J. D. Zuegel, Phys. Plasmas **22**, 110501 (2015).
13. J. Lindl, O. Landen, J. Edwards, and E. Moses, Phys. Plasmas **21**, 020501 (2014).
14. J. D. Moody, B. J. MacGowan, J. E. Rothenberg, R. L. Berger, L. Divol, S. H. Glenzer, R. K. Kirkwood, E. A. Williams, and P. E. Young, Phys. Rev. Lett. **86**, 2810 (2001).
15. R. Betti and O. A. Hurricane, Nat. Phys. **12**, 435 (2016).
16. D. Batani, S. Baton, A. Casner, S. Depierreux, M. Hohenberger, O. Klimo, M. Koenig, C. Labaune, X. Ribeyre, C. Rousseaux, G. Schurtz, W. Theobald, and V. Tikhonchuk, Nucl. Fusion **54**, 054009 (2014).
17. G. Cristoforetti, L. Antonelli, D. Mancelli, S. Atzeni, F. Baffigi, F. Barbato, D. Batani, G. Boutoux, F. D'Amato, J. Dostal, R. Dudzak, E. Filippov, Y. J. Gu, L. Juha, O. Klimo, M. Krus, S. Malko, A. S. Martynenko, Ph. Nicolai, V. Ospina, S. Pikuz, O. Renner, J. Santos, V. T. Tikhonchuk, J. Trela, S. Viciani, L. Volpe, S. Weber, and L. A. Gizzi, High Power Laser Sci. Eng. **7**, e51 (2019).
18. O. Klimo, S. Weber, V. T. Tikhonchuk, and J. Limpouch, Plasma Phys. Control. Fusion **52**, 055013 (2010).
19. Y. J. Gu, O. Klimo, P. Nicola, S. Shekhanov, S. Weber, and V. T. Tikhonchuk, High Power Laser Sci. Eng. **7**, e39 (2019).
20. S. Weber, C. Riconda, and V. T. Tikhonchuk, Phys. Rev. Lett. **94**, 055005 (2005).

https://doi.org/10.1017/hpl.2020.22 Published online by Cambridge University Press

21. L. Lancia, J. R. Marques, M. Nakatsutsumi, C. Riconda, S. Weber, S. Hüller, A. Mančić, P. Antici, V. T. Tikhonchuk, and A. Héron, Phys. Rev. Lett. **104**, 025001 (2010).
22. B. Rethfeld, D. S. Ivanov, M. E. Garcia, and S. I. Anisimov, J. Phys. D: Appl. Phys. **50**, 193001 (2017).
23. D. Price, R. More, R. Walling, G. Guethlein, R. Shepherd, R. Stewart, and W. White, Phys. Rev. Lett. **75**, 252 (1995).
24. K. M. George, J. T. Morrison, S. Feister, G. K. Ngirmang, J. R. Smith, A. J. Klim, J. Snyder, D. Austin, W. Erbsen, K. D. Frische, J. Nees, C. Orban, E. A. Chowdhury, and W. M. Roquemore, High Power Laser Sci. Eng. **7**, e50 (2019).
25. Y. Zhao, J. Zheng, M. Chen, L. L. Yu, S. M. Weng, C. Ren, C. S. Liu, and Z. M. Sheng, Phys. Plasmas **21**, 112114 (2014).
26. A. Ghizzo, T. W. Johnston, T. Réveillé, P. Bertrand, and M. Albrecht-Marc, Phys. Rev. E **74**, 046407 (2006).
27. C. F. Wu, Y. Zhao, S.-M. Weng, M. Chen, and Z.-M. Sheng, Acta Phys. Sin. **68**, 195202 (2019).
28. C. Riconda, S. Weber, V. Tikhonchuk, J.-C. Adam, and A. Heron, Phys. Plasmas **13**, 083103 (2006).
29. M. N. Rosenbluth, Phys. Rev. Lett. **29**, 565 (1972).
30. C. S. Liu, M. N. Rosenbluth, and R. B. White, Phys. Fluids **17**, 1211 (1974).
31. R. A. Fonseca, L. O. Silva, F. S. Tsung, V. K. Decyk, W. Lu, C. Ren, W. B. Mori, S. Deng, S. Lee, T. Katsouleas, and J. Dongarra, in *International Conference on Computational Science* (Springer, 2002), p. 342.
32. R. G. Hemker, arXiv:1503.00276 (2015).
33. Y. Zhao, Z. Sheng, S. Weng, S. Ji, and J. Zhu, High Power Laser Sci. Eng. **7**, e20 (2019).
34. T. Z. Esirkepov, F. F. Kamenets, S. V. Bulanov, and N. M. Naumova, JETP Lett. **68**, 36 (1998).
35. S. V. Bulanov, T. Z. Esirkepov, N. M. Naumova, F. Pegoraro, and V. A. Vshivkov, Phys. Rev. Lett. **82**, 3440 (1999).
36. Y. Sentoku, T. Z. Esirkepov, K. Mima, K. Nishihara, F. Califano, F. Pegoraro, H. Sakagami, Y. Kitagawa, N. M. Naumova, and S. V. Bulanov, Phys. Rev. Lett. **83**, 3434 (1999).
37. N. Naumova, S. Bulanov, T. Esirkepov, D. Farina, K. Nishihara, F. Pegoraro, H. Ruhl, and A. Sakharov, Phys. Rev. Lett. **87**, 185004 (2001).
38. D. Wu, W. Yu, S. Fritzsche, C. Y. Zheng, and X. T. He, Phys. Plasmas **26**, 063107 (2019).

https://doi.org/10.1017/hpl.2020.22 Published online by Cambridge University Press